Soft Matter

Cite this: *Soft Matter*, 2012, **8**, 8113

www.rsc.org/softmatter

PAPER

Magnitude and presentation of mechanical signals influence adult stem cell behavior in 3-dimensional macroporous hydrogels†

Ross A. Marklein, Danielle E. Soranno and Jason A. Burdick*

Received 2nd March 2012, Accepted 13th April 2012
DOI: 10.1039/c2sm25501d

The mechanical properties of the microenvironment are being recognized as a key contributor to stem cell behaviour, whether in the context of tissues or when designing biomaterials. While there has been considerable evidence demonstrating the effect of 2-D static mechanics on stem cells, few systems exist to investigate the influence of the 3-D presentation of mechanical signals. In this study, methacrylated hyaluronic acid (MeHA) was processed into porous (crosslinking around spherical templates) 3-D hydrogels with tunable elastic moduli ranging from ~1.5 kPa to 12.4 kPa. Porous hydrogels were fabricated with a sequential crosslinking process (addition crosslinking of methacrylates with dithiols, followed by UV photopolymerization) where the hydrogel mechanics are controlled by the extent of UV exposure and are subsequently seeded with human mesenchymal stem cells (hMSCs). hMSCs spread within the pores and proliferated in a mechanically dependent manner as cells within the softest 1.5 kPa hydrogels were less spread initially and showed little proliferation with time, while hMSCs in stiffer hydrogels (>1.5 kPa) had higher initial spreading and a roughly two-fold increase in cell number after 14 days. In growth media, porous hydrogels supported a slight upregulation (two to eight-fold) in chondrogenic genes across all mechanics, while there was only modest upregulation in a few conditions (and in many cases downregulation) for myogenic, osteogenic, and adipogenic genes. The secretion of various cytokines and angiogenic molecules was found to be mechanically dependent in the porous system with greater secretion at day 2 in the stiffer hydrogels (3.8 kPa and 7.4 kPa). However, by day 14 there was greater secretion in the softer hydrogels (1.5 kPa and 2.6 kPa). Finally, when mechanics were temporally increased during culture (from ~2.6 kPa to 12.4 kPa), there was a noticeable decrease in the secretion of 15 angiogenic and cytokine proteins. Thus, the influence of mechanics on stem cells within hydrogel structures appears to be dependent on the magnitude and timing of presentation.

Introduction

In order to effectively incorporate stem cells into therapeutic applications, it is important to thoroughly understand the microenvironmental factors that influence stem cell behaviour.[1] For example, the effect of substrate mechanics on stem cells has received considerable attention due to the ability of mechanics to control cell morphology, proliferation, differentiation, and molecule secretion.[1–3] Human mesenchymal stem cells (hMSCs) have well documented mechanosensitive behaviour[2,4,5] and have been implemented in therapeutic strategies due to their ability to differentiate into many cell types, as well as to produce potentially therapeutic factors.[6] Thus, to effectively utilize hydrogels as synthetic environments in tissue engineering applications or as extracellular matrix mimics to understand how stem cells behave in controlled environments, a greater understanding of how MSCs respond to 3-dimensional hydrogel mechanics is necessary.

A plethora of natural and synthetic hydrogels have been used to understand mechanical influences on cells.[1] However, few systems possess the ability to spatially and temporally control mechanics[5,7–9] despite the distinct mechanical heterogeneity that exists in many pathologies (*e.g.*, post-myocardial infarction, calcification and fibrosis in heart valves),[10,11] as well as during tissue development.[12] Additionally, few studies present hydrogels in a 3-D context, rather using hydrogels as simple 2-D substrates. The few studies on 3-D stem cell mechanosensitivity include systems such as static alginate gels of varied crosslink density[4] and photodegradable gels with tunable mechanics.[13] Thus, there still exists the need for advanced material systems to further investigate complex mechanical environments in more biologically relevant 3-D contexts.

We previously developed a sequential crosslinking process[5] for hydrogel fabrication that relies on both the Michael addition crosslinking of methacrylated hyaluronic acid (MeHA) with

Department of Bioengineering, University of Pennsylvania, 240 Skirkanich Hall, 210 S. 33rd Street, Philadelphia, PA, 19104 USA. E-mail: burdick2@seas.upenn.edu; Fax: +215-573-2071; Tel: +215-898-8537

† Electronic Supplementary Information (ESI) available: values for secretory profile raw data. See DOI: 10.1039/c2sm25501d/

a dithiol molecule and then the subsequent light-initiated radical polymerization of remaining methacrylates, where light provides control over both the timing and spatial presentation of the secondary crosslinking process. HA not only presents the appropriate chemistry for sequential crosslinking, but it is also present in many tissues and involved in processes such as wound healing, cell motility, inflammation, and embryonic development.[14–16]

In this work, the sequential crosslinking system was translated to a 3-D mechanically-tunable system, where gelation occurs around a bead template, leading to macroporous structures where cells can be seeded through the pores with a range of mechanical properties. This hydrogel system allows for further insight into hMSC behaviour over a physiological range of mechanics (1.5–12.4 kPa) in a 3-D macroporous context, as well as a unique method for studying hMSC response to dynamic mechanics (matrix stiffening). There have been initial studies investigating the effects of pore morphology, mechanics, and adhesivity on MSC motility,[14] however further investigation into other complex stem cell responses is necessary. The results of these studies demonstrate the importance of the magnitude and presentation of mechanics on hMSC morphology, proliferation, differentiation, and molecule secretion. Finally, this macroporous hydrogel system provides advantages over other mechanically-tunable systems as it can serve as a desirable tissue engineering platform due to its high degree of tunability, as well as the benefits imparted by a porous architecture (high water content and potential for cell infiltration).

Experimental

MeHA synthesis and characterization

MeHA was synthesized as outlined previously in order to obtain a macromer with ~100% modification (% methacrylation).[5] Modification efficiency was defined as the percentage of HA repeat units containing methacrylates based on ^{1}H NMR. Briefly, a 1 wt% solution of sodium hyaluronate (Lifecore, 59 kDa) in dIH_2O was reacted with methacrylic anhydride (2.4 mL g^{-1} HA) at 4 °C for 8 h while maintaining pH 8 using 5 N NaOH. Following overnight stirring at 4 °C, additional methacrylic anhydride was added (1.2 mL g^{-1} HA) and reacted for 4 h. The solutions were dialyzed for 4 days, frozen overnight at −80 °C, and lyophilized.

Hydrogel fabrication and morphological characterization

For the sequentially crosslinked hydrogel system, a 3 wt% MeHA solution dissolved in 0.2 M triethanolamine (TEA) at pH 9 was reacted with dithiothreitol (5 mM) in order to "consume" ~15% of the methacrylates (Fig. 1A 'Addition') for 2 h at 37 °C. In order to vary the crosslink density, a solution of 0.05% I2959 (Irgacure) was then incubated with the hydrogels for 1 h, followed by a range of UV exposure times (up to 2 min) using 10 mW cm^{-2} collimated UV light (Omnicure S1000 UV Spot Cure Systems), where the time of light exposure controlled the extent of secondary crosslinking. The compressive moduli of non-porous hydrogels were determined using a Dynamic Mechanical Analyzer (DMA, TA Instruments). A mechanical testing regimen of 10% strain/min was used and the compressive modulus for each hydrogel was determined by evaluating the stress-strain slope between 5% and 20% strain (n = 4 hydrogels/group).

Porous hydrogels were fabricated using a similar approach, but the addition crosslinking solution was pipetted onto a cylindrical PMMA microsphere template (Polysciences, Inc. average diameter of beads ~250 μm) with diameter 7.5 mm and thickness 2.3 mm that had been sonicated to introduce hexagonal close packed order (Fig. 1B). Following incubation for 2 h at 37 °C, the hydrogel/template constructs were serially washed to dissolve the beads (3× Acetone, 3× EtOH, 3× PBS). After the final PBS wash, a solution of 0.05% I2959 solution was introduced in order to perform the secondary 'radical crosslinking'. Following UV exposure (0–120 s), the porous hydrogels were again washed in PBS (to remove excess I2959). The compressive modulus of porous samples was determined as above. In order to characterize the porous morphology of the hydrogels, a 10 μM solution of thiolated-FITC (Toronto Research Chemicals, Inc.) was diffused into the hydrogels for 1 h and then rinsed 3X with PBS. Porous hydrogels were imaged using a two-photon confocal microscope (Zeiss LSM510) and pore diameter calculated for each mechanics group using ImageJ (n = 20 pores/hydrogel, n = 3 hydrogels/group). The same confocal stacks were also threshold adjusted in order to determine the porosity of the hydrogels for each condition (n = 5 slices/hydrogel, n = 3 hydrogels/group) using ImageJ. The porosity was then used to evaluate compressive moduli of both non-porous and porous hydrogels using the Gibson-Ashby model for open cell foam structures shown in eqn (1).[15]

$$E^* = (\rho^*/\rho_s)E_s \quad (1)$$

E^* represents the modulus of the porous material, E_s the modulus of the material when non-porous, and (ρ^*/ρ_s) the ratio of the porous and non-porous densities (calculated as stated above using ImageJ).

Porous hydrogel preparation for cell culture

As above, porous hydrogels were fabricated using microsphere templates and targeting ~15% methacrylate consumption with DTT followed by secondary UV exposure to alter the crosslink density. Prior to addition crosslinking, the adhesive oligopeptide GCGYG*RGD*SPG was coupled to the MeHA backbone (1 mM RGD) using the same 'addition reaction' method. While the RGD peptide binds to methacrylates that would otherwise be consumed by Michael Addition or radical crosslinking, the percentage of methacrylates consumed (assuming 100% coupling efficiency) was only ~1% for this coupling process and RGD concentration used. Prior to cell-seeding, samples were sterilized using germicidal UV for 1 h, and pre-incubated with growth medium. Growth medium consisted of the base medium α-MEM, 20% FBS, 1% L-glutamine, and 1% Pen-Strep (Gibco for all components). 125 000 hMSCs (Lonza, passage 3) were pipetted onto each side of the porous hydrogels (Fig. 1B, 250 000 hMSCs total) and cultured for 14 days in growth medium. In order to investigate hMSC response to dynamic (step-wise increase) mechanics, 0.05% I2959 solution was added to 2.6 kPa hydrogel groups on day 2 and day 7 of cell culture for 1 h and

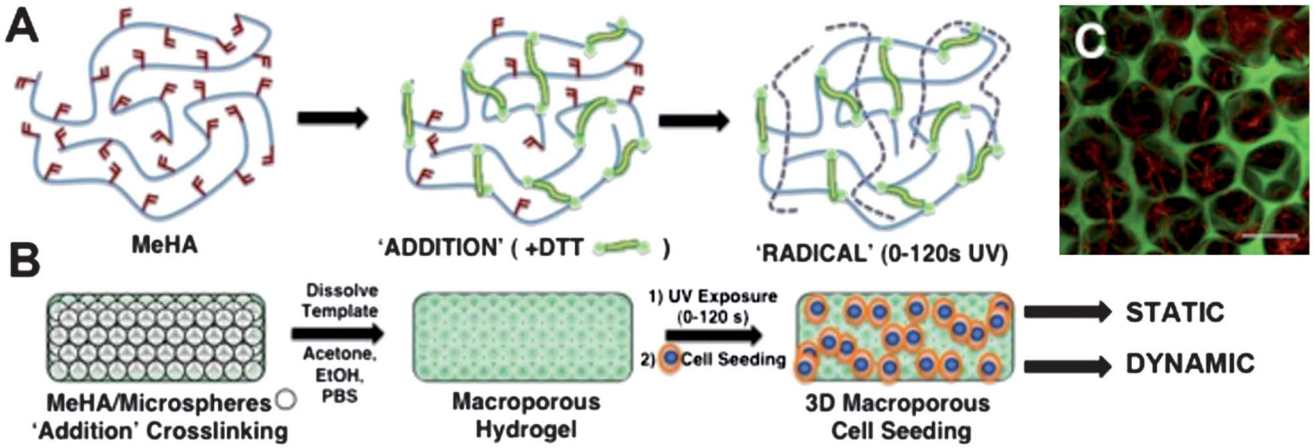

Fig. 1 (A) Schematic of sequential crosslinking process used for the fabrication of hydrogels with varying crosslinking. Methacrylates are first consumed using a dithiol crosslinker (DTT) *via* a Michael Addition ('Addition') reaction. Remaining methacrylates can be further crosslinked using UV light in the presence of photoinitiator (kinetic chains shown with dotted lines, 'Radical'). (B) Addition crosslinking of MeHA around a PMMA microsphere template results in a porous hydrogel architecture following microsphere leaching by solvent exchanges (acetone, ethanol, PBS). Following template removal, the mechanics are tuned by introducing photoinitiator (I2959) and varying UV exposure time (0–120 s). Cells are then seeded on both sides of the porous hydrogel and cultured with static or dynamic mechanics (by performing further radical crosslinking once the cells are seeded). (C) Representative image of hMSCs (actin, red) within porous hydrogels (FITC-coupled, green). Scale bar = 200 μm.

then exposed to UV for 80 s. Following UV exposure, hydrogels were washed 3× with growth medium (30 s per wash) to remove excess initiator.

Cell morphology and proliferation quantification

hMSC morphology was assessed using rhodamine-phalloidin staining on days 2, 7, and 14 for all hydrogel conditions. Cells were fixed in 10% formalin for 10 min, permeabilized with 0.25% Triton-X for 10 min, and stained with rhodamine-phalloidin for 40 min with 3× PBS washes after each step. Cells were imaged using a Zeiss LSM510 confocal microscope. Cell proliferation was quantified using the PICOGREEN dsDNA assay on days 2, 7, and 14 for all conditions. Samples (n = 4) were placed in CellLytic (Sigma) solution for 1 h and vortexed gently at 37 °C. Samples were measured on a TECAN - InfiniteM200 plate reader and compared with a dsDNA standard curve in order to determine the total DNA content.

Gene expression and secretory profile characterization

In order to assess cell differentiation, RNA was extracted from each sample (n = 4) using Trizol reagent (Invitrogen) and a manual tissue grinder. RNA was reverse-transcribed into cDNA and PCR was performed on the following genes: Collagen II (COL2) and SOX9 (chondrogenic), α-Smooth Muscle Actin (aSMA) and Calponin (CALP) (myogenic), Osteocalcin (OC) and Alkaline Phosphatase (ALP) (osteogenic), Fatty-Acid Binding Protein (FABP) and Peroxisome Proliferator-Activated Receptor γ (PPARG) (adipogenic). Using GAPDH as a housekeeping gene, relative gene expression was determined using the $\Delta\Delta C_T$ method and all experimental values are plotted relative to the day 0 undifferentiated hMSCs seeded into each hydrogel. Note that C_T for GAPDH were consistent between all groups and controls (data not shown).

hMSC secretory profiles were characterized for both angiogenesis and cytokine factors (R&D Systems, kits ARY005 and ARY007) by collecting culture media on days 2, 7, and 14 and pooling for each condition (n = 3). The protein arrays were threshold adjusted and analyzed using a protein array analyzer (ImageJ, NIH) to quantify pixel intensity. Each value was then normalized to the max expression of that protein and plotted in descending order with the protein most highly expressed plotted at the top and proteins minimally expressed plotted at the bottom.

Statistics

Statistics were performed using One-Way and Two-Way ANOVA and Tukey's post-hoc test (R, Free Software Foundation) for hydrogel mechanics, hydrogel pore sizes, cell proliferation, and gene expression studies.

Results and discussion

MeHA hydrogel mechanical characterization

We used a sequential crosslinking process to obtain a wide range of crosslinking densities from the same starting material, by altering the extent of methacrylate polymerization in already formed networks using UV light exposure. Compressive moduli were obtained for bulk non-porous hydrogels (containing RGD peptide) formed with this sequential crosslinking system (scheme illustrated in Fig. 1A) using DMA and are reported in Fig. 2. A range of moduli from 1.5 kPa (no UV exposure) to 7.4 kPa (120 s UV exposure) was obtained by varying the UV exposure time during the secondary radical crosslinking step (Fig. 2A). This represents a simple process to alter hydrogel mechanics to form materials with mechanics that encompass a wide range of tissues.[16]

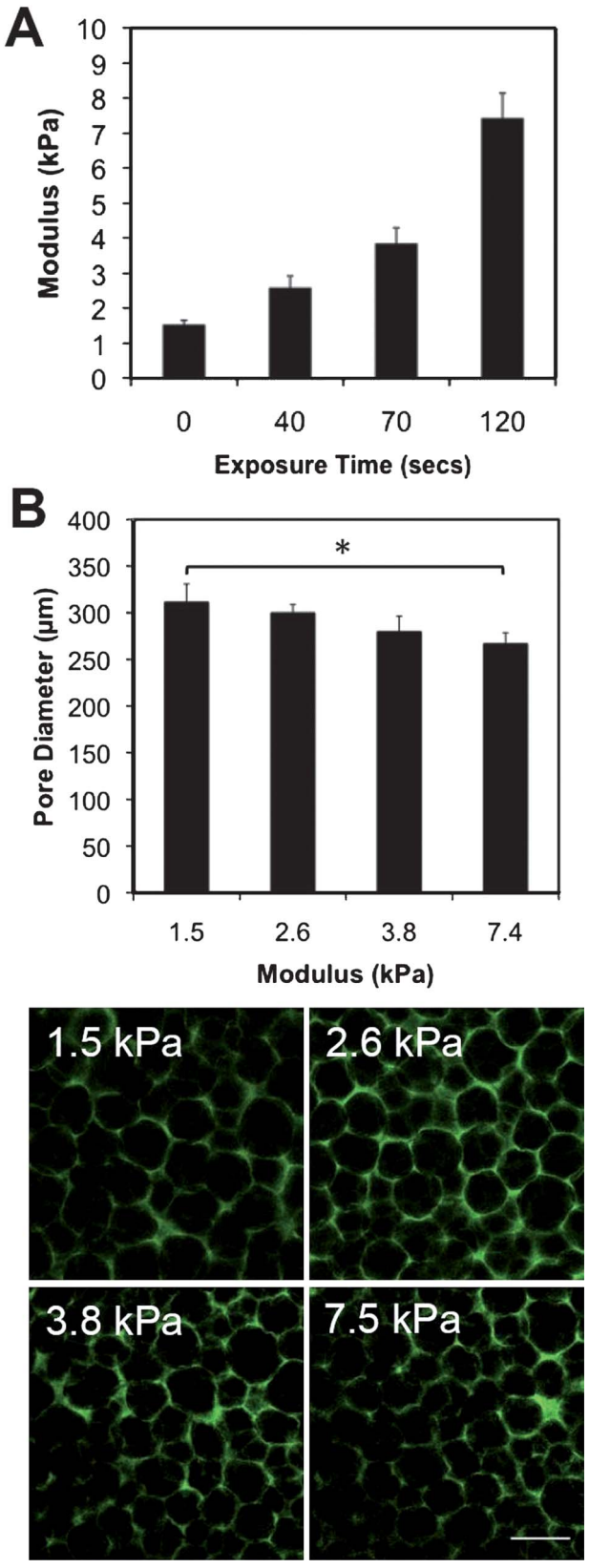

Fig. 2 (A) Hydrogel compressive moduli for bulk sequentially crosslinked hydrogels (0–120s UV exposure range). Statistically significant differences were observed between all groups. (B) Average pore sizes and representative images for macroporous hydrogels with varied crosslinking. Scale bar = 400 μm Significant differences *$p < 0.05$.

Due to the porosity and low crosslinking, the bulk mechanics of the porous hydrogels were difficult to measure using the DMA for groups below the stiffest condition (7.4 kPa, 120 s UV exposure). The bulk compressive modulus of this formulation in a porous architecture measured ~0.2 kPa, which agrees well with the Gibson-Ashby model given our measured porosity of ~85% (as determined using threshold adjusted confocal images, example shown in ESI,† Fig. S1). Given that the moduli of both porous (0.2 kPa) and non-porous (7.4 kPa) hydrogels fit the model for open cell foam mechanics, we are confident that the moduli of the non-porous bulk hydrogels were representative of the microscale moduli experienced by the hMSCs at each porous hydrogel formulation. This local modulus is most relevant as this is what the cell experiences during adhesion, spreading, and traction-mediated behaviour.

Due to the highly swollen nature of porous hydrogels, the average pore size was calculated for each mechanics group and shown in Fig. 2B with representative images of the porous architecture for varied light-exposure. While there was a significant difference between the pore size in the softest (1.5 kPa) and stiffest (7.4 kPa) conditions, this difference in pore size (310 μm *vs.* 270 μm, respectively) likely has a minimal affect on cell behaviour because the pore size scale (hundreds of μm) is much larger than that of cells (tens of μm). However, these differences between the softest and stiffest groups must be considered in the context of the results of this study. In one particular study investigating the effects of porous hydrogel mechanics, pore sizes on the order of cell diameters (7–20 μm) were used to demonstrate the influence of porous architecture on MSC motility.[14] Our study similarly utilized a mechanically-tunable porous system, however we further investigated the effects of 3-D porous mechanics on other stem cell responses (morphology, proliferation, differentiation, and secretion), as well as the effects of dynamic mechanics.

hMSC morphology and proliferation response to mechanics

Stem cell morphology and proliferation exhibited mechano-dependence in porous hydrogels as shown in Fig. 3. Cells exhibited increased spreading and a more organized actin cytoskeleton with increasing mechanics on day 2 (Fig. 3A), which agrees well with previous findings in 2-D systems.[5,17] Due to the macroporous scaffold morphology, this system represents a quasi-2D presentation of mechanics that directs the formation of a complex 3-D environment for the cells seeded within the hydrogel. By day 7, cells in the 2.6, 3.8, and 7.4 kPa groups had similar confluent morphologies with cells filling the scaffold pores as opposed to the cells in 1.5 kPa gels, which had begun to contract the scaffold and a distinct cell mass was apparent.

Although there was an increase in DNA with time above a threshold mechanics of 2.6 kPa, there was no significant difference in DNA content at any of the time points among the 2.6, 3.8, and 7.4 kPa groups, potentially due to the high seeding density and cell-cell interactions. Contact inhibition of proliferation is apparent in stem cell culture once confluency is reached[18] and this could contribute to the lack of differences observed in cell number between the groups above 1.5 kPa as the cells completely fill the pores by day 7. Furthermore, there was no significant increase in DNA with the 1.5 kPa with culture, which

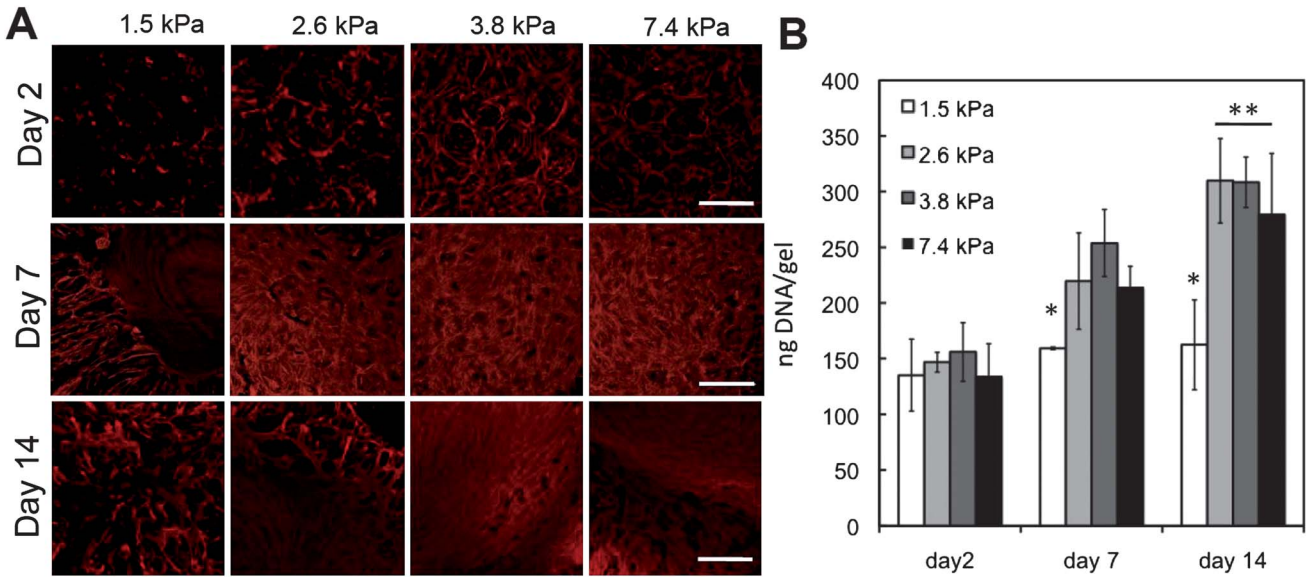

Fig. 3 (A) hMSC morphology/cytoskeletal organization (actin, red) in porous hydrogels at day 2, 7, and 14. (B) Cell numbers (represented with DNA content) with culture time in the various macroporous hydrogels. Statistically significant differences were observed between '1.5 kPa' and all other groups at days 7 and 14 (*$p < 0.01$) and with hydrogels at a given mechanics between day 2 and day 14 (**$p < 0.001$). Scale bar = 400 μm.

was significantly lower at the 7 and 14 day time points than all other groups (Fig. 3B). Although the observed contraction in 1.5 kPa gels and the proliferation/confluency of the other groups resulted in differences in cell-scaffold and cell-cell interactions with time (as well as an accompanied decrease in porosity), the initial mechanical cue provided by the porous hydrogels played a role in the resulting stem cell behavior. It was not possible to directly measure the hydrogel mechanics in the presence of cells during the experiment and any cell produced matrix could also influence local interactions with the gel.

hMSC lineage marker expression in response to mechanics

hMSC expression of lineage markers was evaluated after 14 days in growth medium for four common hMSC fates: chondrogenesis, myogenesis, osteogenesis, and adipogenesis. The growth media does not include inductive components to specifically induce differentiation in cells. The only notable upregulation in genes (relative to day 0 hMSCs) occurred for the chondrogenic and adipogenic markers: Col2 (two- to three-fold) and Sox9 (four- to eight-fold) for chondrogenesis and FABP (two-fold) for adipogenesis. Because the cells are cultured in growth media, changes in gene expression are likely due to morphology, proliferation, and cell-cell contacts imposed by differential mechanics and the porous architecture.

There were no significant differences between groups for the chondrogenic genes; however, FABP and PPARG expression significantly differed between 1.5 kPa and all other mechanics (Fig. 4). Although osteocalcin expression was highest in the softest hydrogels (contrary to 2-D findings),[2] studies have demonstrated increased upregulation in softer 3-D hydrogels that allow for scaffold contraction and reduced proliferation.[19,20] The increased cell-scaffold compaction also resulted in enhanced cell-cell contact, which has been correlated with chondrogenesis in cell pellet cultures.[21] There were also observed differences in myogenic marker aSMA and CALP expression, with the 1.5 kPa group exhibiting greater downregulation (five-fold and twenty-fold for aSMA and CALP, respectively, compared to day 0 hMSCs) while the other mechanics groups did not exhibit as drastic of downregulation of these myogenic markers. Softer hydrogels (~1 kPa) have demonstrated reduced myogenic potential for hMSCs cultured in growth medium (in the presence and absence of TGFβ) coupled with enhanced chondrogenesis,[22] which correlates well with the differentiation profile observed for stem cells cultured in 1.5 kPa porous hydrogels. Thus, there is evidence that the outlier in spreading and proliferation (*i.e.*, 1.5

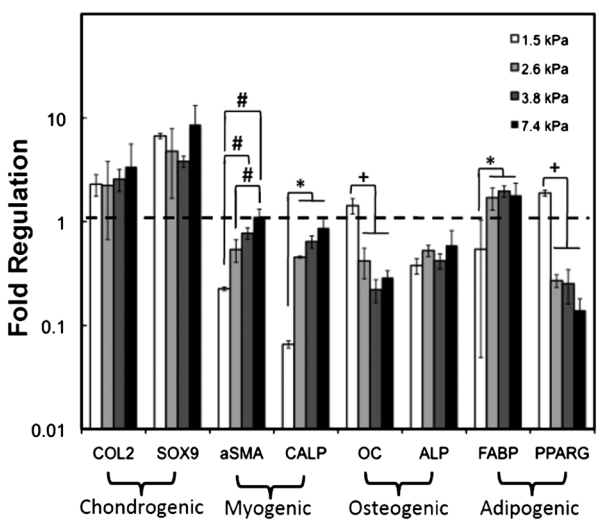

Fig. 4 Day 14 expression of various genes for hMSCs cultured in porous hydrogels. Values above dotted line indicate upregulation relative to d0 hMSCs. Statistically significant differences: *$p < 0.05$, #$p < 0.01$, +$p < 0.001$.

kPa) exhibits differences in differentiation marker expression influenced by the initial porous hydrogel mechanics.

hMSC secretory profile response to mechanics

Collected medium was analyzed for 55 angiogenesis and 36 cytokine factors using proteome profile arrays and results for each mechanics group are plotted in Fig. 5. There was a general increase in angiogenic/cytokine factor expression for the softer hydrogels 1.5 kPa and 2.6 kPa with time (Fig. 5, data reported in ESI,† Fig. S2). There was maximal expression in the softer hydrogels at day 14 for 9 factors (IL-8, IL-6, GROalpha, MIF, CXCL16, Thrombospondin-1, GDNF, GM-CSF, and G-CSF). With the stiffer hydrogels (3.8 kPa and 7.4 kPa), there was initially a greater overall expression at day 2 for several factors followed by a noticeable decrease by day 14, such as MMP-9, Ang-1, Ang-2, Endothelin-1, Activin A, Serpin B5 and EG-VEGF. There were also only 2 maximally expressed proteins (MCP-1, IGFBP-1) on the stiffer hydrogels at day 14. Temporal changes in trophic factor secretion have also been demonstrated in 2-D hydrogel systems,[3] where stiffer substrates (~20 kPa) have been shown to initially support greater factor secretion while after 2 weeks the secretion profiles shift to greater secretion on softer hydrogels (~2 kPa). Also of note, the angiogenic factors PlGF and Angiogenin exhibited profiles with both temporal and mechanical dependence as they were transiently expressed on 2.6 kPa gels at day 7, but minimally detected on other days and on other mechanics. With respect to changes in secretory molecules on a per cell basis, the only groups that had statistically different cell numbers were the softest hydrogel and all other groups at days 7 and 14. This further amplifies the findings, as the softest group had the highest total values for many molecules at these later times.

While the porous hydrogel system did not afford a group with uniformly high factor secretion, the secretome profiles showed distinct temporal behaviour based on the initial scaffold mechanics. In tissue engineering applications, the timing of stem cell injection is of critical importance[23,24] and further investigation into the effect of mechanics on not only the factors secreted, but also their temporal expression is necessary. These results reinforce the importance of the mechanics magnitude and presentation on cell behaviour with respect to the production and release of molecules from cell-hydrogel constructs.

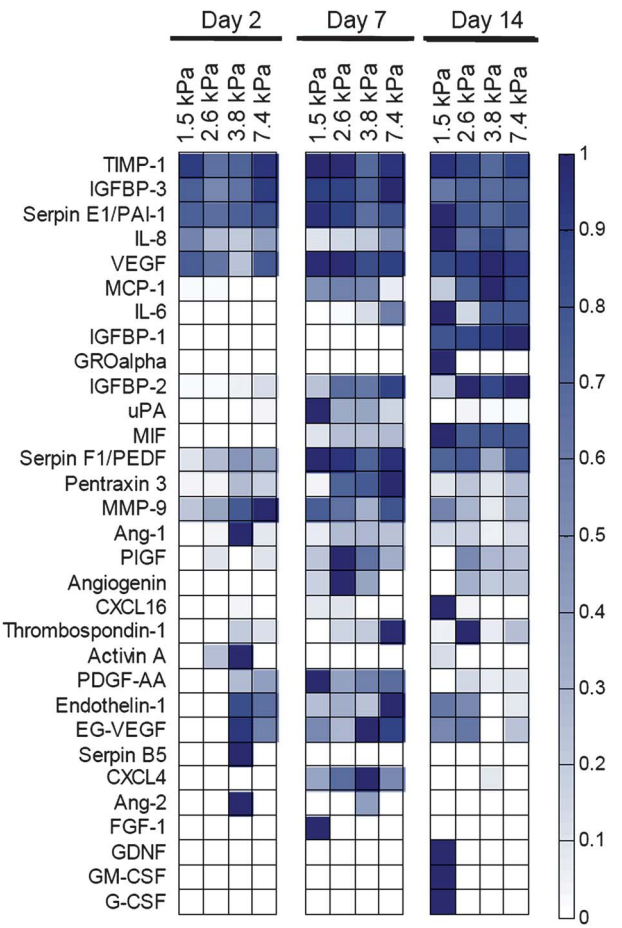

Fig. 5 Secretory profiles for angiogenic and cytokine factors by hMSCs interacting with porous hydrogels at days 2, 7, and 14. Molecule expression is normalized to the maximum detected expression. Molecules are then plotted with those having the highest maximal expression at the top and those with minimal detection at the bottom. Normalized colorimetric scale bar displayed on the right.

hMSC response to dynamic mechanics

In addition to providing a means to alter mechanical properties in constructs, the sequential crosslinking technique can also temporally alter mechanical properties when the light exposure occurs at a later time point after cell seeding. In this example, this leads to a step-wise increase in mechanical properties. Fig. 6A demonstrates the ability of this hydrogel system to "stiffen" by exposing an initially soft 2.6 kPa hydrogel ('static') to an additional 80 s of UV (120 s total UV exposure, 'dynamic') in order to significantly increase the modulus to 12.4 kPa. The intermediate modulus group of 2.6 kPa was chosen as the group to be stiffened because it represented the threshold mechanics above which cell morphology and proliferation did not show significant differences. While the stiffened condition of 12.4 kPa did not match the static condition with the highest modulus (7.4 kPa), the ability to dramatically increase the hydrogel mechanics still allowed for insight into the effects of dynamic mechanics on stem cell behaviour in 3-D. hMSC photoencapsulation under similar crosslinking conditions has been well established and shown to not diminish cell viability,[21,25,26] and recent work performed in a similar 2-D stiffened system has demonstrated minimal effect of delayed UV exposure on cell viability.[27]

There were no significant differences in cell proliferation and morphology (Fig. 6B and 6C), which agreed well with previous results for the static hydrogels (Fig. 3) above the 2.6 kPa threshold. Like the static mechanics conditions, cell DNA content increased roughly twofold by day 14 for unstiffened and stiffened conditions and cells spread and became confluent throughout the porous hydrogels. Furthermore, there were no significant differences in cell differentiation for either of the stiffening conditions (day 2 or day 7) as compared to the non-stiffened 2.6 kPa condition (Fig. 6D), which also agreed with the static mechanics results above this threshold mechanics (Fig. 4A). In terms of cell viability, Alamar Blue results (ESI,† Fig. S3) demonstrated no significant differences in cell metabolic

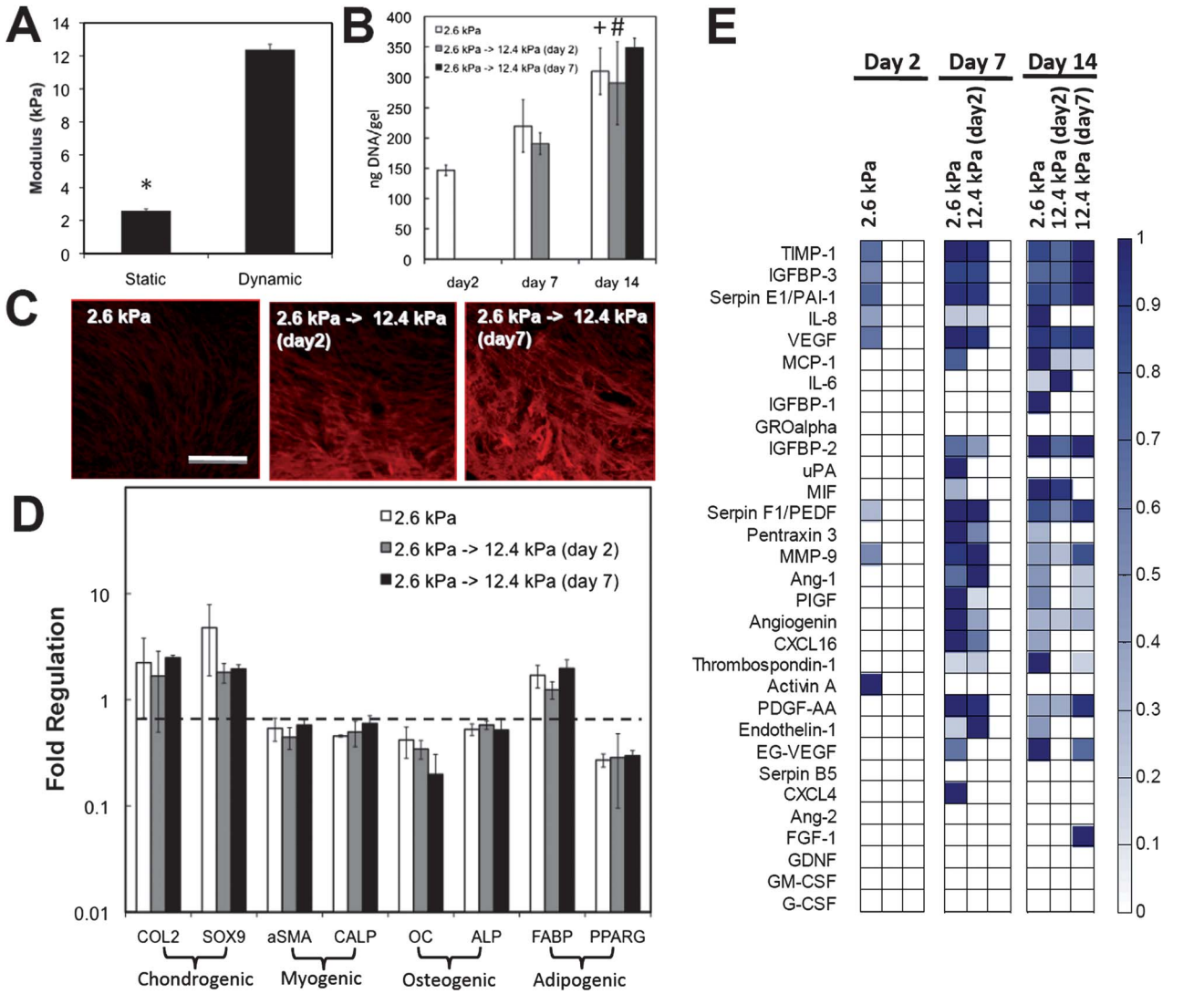

Fig. 6 (A) Dynamic mechanics as measured by DMA. Significant differences between stiffened (12.4 kPa) and unstiffened (2.6 kPa) conditions * $p < 0.001$ (B) Cellular DNA content over time in dynamic hydrogels. Significant differences in 2.6 kPa hydrogels from day 2 to day 14 (+$p < 0.01$) and in 12.4 kPa-day 2 stiffened hydrogels from day 7 to day 14 (#$p < 0.05$). (C) Cell morphology in dynamic hydrogels (actin, red) at day 14. Scale bar = 400 μm (D) Day 14 hMSC gene expression (normalized to day 0 hMSCs) and (E) secretory profiles plotted with maximally expressed proteins at the top and minimally expressed proteins at the bottom. Values are normalized to maximum expression of unstiffened 2.6 kPa hydrogels and stiffened hydrogels (day 2 and day 7) only. Normalized colorimetric scale bar displayed on the right.

activity under any of the stiffening conditions (and at any time point) further exemplifying that our *in situ* UV exposure does not have deleterious effects on the hMSCs. Our previous work also indicates that the exposure of the cells to this intensity and time of UV light and the photoinitiator does not have detrimental effects on cell viability.[27]

While the morphology, proliferation, and differentiation responses to dynamic mechanics do not reveal a significant stem cell response to dynamic mechanics (due to the range selected), the secretory profiles demonstrate otherwise. As shown in Fig. 6E (data reported in ESI,† Fig. S4), there were overall decreases in stem cell angiogenic and cytokine factor expression for all stiffening conditions on both day 7 and day 14. On day 7, the hydrogels stiffened on day 2 had reduced expression of 12 proteins: Angiogenin, CXCL16, EG-VEGF, IGFBP-1 and −2, MCP-1, Pentraxin 3, CXCL4, PlGF, IL-8, MIF and uPA. On day 14, there was an even greater difference in factor secretion between unstiffened 2.6 kPa hydrogels and day 2 stiffened 12.4 kPa hydrogels. Nearly every protein with diminished expression on day 7 (with the exception of uPA and CXCL4) also exhibited lower expression at day 14 along with Ang-1, Endothelin-1, MMP-9, Serpin F1, and Thrombospondin-1. The secretory profile for hMSCs in day 7 stiffened 12.4 kPa hydrogels also showed diminished factor secretion compared to unstiffened 2.6 kPa hydrogels at day 14, but not quite as different as in the day 2 stiffened 12.4 kPa condition. At day 14, only 10 molecules showed decreased expression for the day 7 stiffened groups when compared to day 2 stiffened hydrogels, which had 15 proteins with reduced expression. This provides evidence for dynamic stem cell responses as cells that were exposed to the stiffer 12.4 kPa microenvironment for longer times showed a greater reduction in angiogenic and cytokine factor expression.

The results of this dynamic culture study implicate mechanics as a profound effector of stem cell angiogenic and cytokine factor secretion. Although there were no significant differences in stem cell morphology, proliferation, and differentiation that resulted from hydrogel stiffening, the differences in secretory profiles can be attributed to dynamic mechanics. This also provides evidence that hMSCs were responsive to the hydrogel mechanics after day 7 even though there is a possibility of ECM deposition during the culture period, which could contribute to a change in local matrix mechanics and stem cell behaviour. Further studies are necessary to determine how hMSCs dynamically sense the changes in mechanics and how this mechanosensing signal results in changes in secretion of specific factors *in vitro* and *in vivo*.

Conclusions

A range of hydrogel mechanics (1.5–12.4 kPa), as well as static and dynamic mechanics, were investigated and shown to influence hMSC behaviour in 3-D macroporous hydrogels. Cell proliferation and morphology in porous hydrogels were mechanosensitive, as cells cultured in hydrogels with modulus >2.6 kPa exhibited greater initial spreading and proliferation over two weeks. Differentiation was also shown to be mechanically-dependent as the expression of several genes differed between the 1.5 kPa hydrogels and all other mechanics groups. Evidence for hMSC secretory profile dependence on mechanics was apparent, as distinct temporal secretion profiles were evident for softer (1.5 and 2.6 kPa) and stiffer (3.8 and 7.4 kPa) hydrogels. hMSC secretion was also temporally modulated by stiffening 2.6 kPa hydrogels at two different time points and found to decrease more drastically when stiffened at an earlier time point (day 2). The results of this study further emphasize the importance of the initial mechanics (magnitude, context, and timing) on stem cell behaviour *in vitro* and how mechanics should be incorporated as a design variable for biomaterials and considered when elucidating stem cell responses *in vivo*.

Acknowledgements

We are grateful for support from a Fellowship in Science and Engineering from the David and Lucile Packard Foundation (JAB) and a CAREER award (JAB) and Graduate Research Fellowship (RAM) from the National Science Foundation.

Notes and references

1 R. A. Marklein and J. A. Burdick, *Adv. Mater.*, 2010, **22**, 175–189.
2 A. J. Engler, S. Sen, H. L. Sweeney and D. E. Discher, *Cell*, 2006, **126**, 677–689.
3 F. P. Seib, M. Prewitz, C. Werner and M. Bornhaeuser, *Biochem. Biophys. Res. Commun.*, 2009, **389**, 663–667.
4 N. Huebsch, P. R. Arany, A. S. Mao, D. Shvartsman, O. A. Ali, S. A. Bencherif, J. Rivera-Feliciano and D. J. Mooney, *Nat. Mater.*, 2010, **9**, 518–526.
5 R. A. Marklein and J. A. Burdick, *Soft Matter*, 2010, **6**, 136–143.
6 A. Behfar, L. V. Zingman, D. M. Hodgson, J.-M. Rauzier, G. C. Kane, A. Terzic and M. Pucéat, *FASEB J.*, 2002, **16**, 1558–1566.
7 A. M. Kloxin, J. A. Benton and K. S. Anseth, *Biomaterials*, 2010, **31**, 1–8.
8 B. M. Gillette, J. A. Jensen, M. Wang, J. Tchao and S. K. Sia, *Adv. Mater.*, 2010, **22**, 686–691.
9 F. X. Jiang, B. Yurke, R. S. Schloss, B. L. Firestein and N. A. Langrana, *Biomaterials*, 2010, **31**, 1199–1212.
10 A. P. Sage, Y. Tintut and L. L. Demer, *Nat. Rev. Cardiol.*, 2010, **7**, 528–536.
11 T. A. Ulrich, E. M. d. J. Pardo and S. Kumar, *Cancer Res.*, 2009, **69**, 4167–4174.
12 P. Patwari and R. T. Lee, *Circ. Res.*, 2008, **103**, 234–243.
13 A. M. Kloxin, A. M. Kasko, C. N. Salinas and K. S. Anseth, *Science*, 2009, **324**, 59–63.
14 S. R. Peyton, Z. I. Kalcioglu, J. C. Cohen, A. P. Runkle, K. J. Van Vliet, D. A. Lauffenburger and L. G. Griffith, *Biotechnol. Bioeng.*, 2011, **108**, 1181–1193.
15 L. J. Gibson and M. F. Ashby, *Cellular Solids: Structure and Properties*, Cambridge University Press, 1999.
16 D. E. Discher, D. J. Mooney and P. W. Zandstra, *Science*, 2009, **324**, 1673–1677.
17 A. S. Rowlands, P. A. George and J. J. Cooper-White, *Am. J. Physiol.: Cell Physiol.*, 2008, **295**, C1037–C1044.
18 H. Majd, P.-J. Wipff, L. Buscemi, M. Bueno, D. Vonwil, T. M. Quinn and B. Hinz, *Stem Cells*, 2009, **27**, 200–209.
19 D.-C. Chen, Y.-L. Lai, S.-Y. Lee, S.-L. Hung and H.-L. Chen, *J. Biomed. Mater. Res., Part A*, 2006, **80A**, 399–409.
20 M. B. Keogh, F. J. O'brien and J. S. Daly, *Acta Biomater.*, 2010, **6**, 4305–4313.
21 C. Chung and J. A. Burdick, *Tissue Eng. A*, 2009, **15**, 243–254.
22 J. S. Park, J. S. Chu, A. D. Tsou, R. Diop, Z. Tang, A. Wang and S. Li, *Biomaterials*, 2011, **32**, 3921–3930.
23 J. C. George, *Transl. Res.*, 2010, **155**, 10–19.
24 N. K. Satija, V. K. Singh, Y. K. Verma, P. Gupta, S. Sharma, F. Afrin, M. Sharma, P. Sharma, R. P. Tripathi and G. U. Gurudutta, *J. Cell. Mol. Med.*, 2009, **13**, 4385–4402.
25 J. A. Burdick and K. S. Anseth, *Biomaterials*, 2002, **23**, 4315–4323.
26 S. Khetan and J. A. Burdick, *Biomaterials*, 2010, **31**, 8228–8234.
27 M. Guvendiren and J. Burdick, *Nature Communications*, 2012, DOI: 10.1038/ncomms1792.